Published in final edited form as:
J Magn Reson Imaging. 2009 July ; 30(1): 18–24. doi:10.1002/jmri.21816.

Inhomogeneous Sodium Accumulation in the Ischemic Core in Rat Focal Cerebral Ischemia by ^{23}Na MRI

Victor E. Yushmanov, PhD[1,*], **Alexander Kharlamov, MD, PhD**[1], **Boris Yanovski, MD**[1], **George LaVerde, MD, PhD**[2], **Fernando E. Boada, PhD**[2], and **Stephen C. Jones, PhD**[1,2,3]

[1]Department of Anesthesiology, Allegheny-Singer Research Institute, Pittsburgh, PA 15212, USA

[2]MR Research Center, Department of Radiology, University of Pittsburgh School of Medicine, Pittsburgh, PA 15213, USA

[3]Department of Neurology, Allegheny-Singer Research Institute, Pittsburgh, PA 15212, USA

Abstract

Purpose—To test the hypotheses that 1) the regional heterogeneity of brain sodium concentration ($[Na^+]_{br}$) provides a parameter for ischemic progression not available from apparent diffusion coefficient (ADC) data, and 2) $[Na^+]_{br}$ increases more in ischemic cortex than in the caudate putamen (CP) with its lesser collateral circulation after middle cerebral artery occlusion in the rat.

Materials and Methods—Twisted projection imaging ^{23}Na MRI was performed at 3 T. $[Na^+]_{br}$ was independently determined by flame photometry. The ischemic core was localized by ADC, by microtubule-associated protein-2 immunohistochemistry, and by changes in surface reflectivity.

Results—Within the ischemic core, the ADC ratio relative to the contralateral tissue was homogeneous (0.63 ± 0.07), whereas the rate of $[Na^+]_{br}$ increase (slope) was heterogeneous ($P < 0.005$): 22 ± 4%/h in the sites of maximum slope vs. 14 ± 1%/h elsewhere (here 100% is $[Na^+]_{br}$ in the contralateral brain). Maximum slopes in the cortex were higher than in CP ($P < 0.05$). In the ischemic regions, there was no slope/ADC correlation between animals and within the same brain ($P > 0.1$). Maximum slope was located at the periphery of ischemic core in 8/10 animals.

Conclusion—Unlike ADC, ^{23}Na MRI detected within-core ischemic lesion heterogeneity.

Keywords

rat brain; focal ischemia; permanent MCAO; ADC; ^{23}Na MRI; tissue sodium

INTRODUCTION

The apparent diffusion coefficient (ADC) of tissue water is an established MRI marker for initial ischemic damage to the brain (1). Because ADC alone is insufficient to characterize stroke severity, the diffusion/perfusion mismatch, i.e., the area showing significant cerebral blood flow (CBF) deficit without corresponding ADC decrease, is commonly regarded as a candidate for tissue salvageability (1,2). Lesion evolution studies (3,4) and quantitative positron emission tomography (5,6) suggested, however, that the mismatch may not accurately estimate 'tissue-at-risk', and that both the ADC-defined ischemic core and the

[*]**Correspondence and reprint requests to:** Victor E. Yushmanov, PhD, Department of Anesthesiology, Allegheny-Singer Research Institute, 320 East North Avenue, Pittsburgh PA 15212-4772, voice: 412-359-4362, fax: 412-359-5288, vyushman@wpahs.org.
[†]*Current address:* UPMC Mercy Hospital, Department of Medicine, Pittsburgh, PA 15219, USA

mismatch area do not have unique flow/metabolism counterparts and may contain brain tissue at various stages of the ischemic process. Additional complications include potential permanent or transient ('pseudonormalization') ADC reversibility, which may be accompanied by selective neuronal loss in the lesion core after early reperfusion (1,3,7). To better characterize the threshold phenomena resulting in the ADC/CBF mismatch in stroke, the region-specific ADC responses to cerebral perfusion deficit have been described previously in different models of focal ischemia in rats (8–10). Novel MRI approaches to monitor the progression of ischemic damage and refine the detection of the ischemic penumbra include mapping of cerebral metabolic rate of oxygen utilization (11), blood-oxygen-level-dependent MRI (12) and pH-weighted MRI (13).

^{23}Na MRI has been considered as a possible marker for brain tissue viability after stroke (14–16). Recently, ^{23}Na MRI has been proposed as a means to determine the stroke onset time for establishing patient eligibility for thrombolytic therapy (17). ^{23}Na MRI timing of stroke is based upon the linear increase in brain sodium concentration ($[Na^+]_{br}$) in affected areas (18,19) in the first several hours. In an earlier study by Jones et al. (17), no comparison of ^{23}Na MRI with ADC was made in a model of cortical stroke not involving caudate putamen (CP). The interest in comparison of different brain regions stems from the presence of collateral circulation in cortex, unlike CP where collateral circulation is absent (20–22).

In this study, we hypothesize that 1) the regional heterogeneity of $[Na^+]_{br}$ increase provides an additional 'functional' parameter for assessing brain ischemia, which is not available from ADC data, and 2) ischemic cortex is characterized by more intense $[Na^+]_{br}$ increase than CP in the rat model of focal ischemic stroke.

MATERIALS AND METHODS

Animal Preparation

Approval for animal use was obtained from the appropriate institutional committee and was consistent with the "Principles of laboratory animal care" (NIH publication No. 86-23, revised 1985). Ten normally fed male Sprague-Dawley rats weighing 320 ± 36 g (mean ± SD) were used. Anesthesia was induced with 3% isoflurane, and maintained with 1.0% to 2.5% isoflurane, 30% oxygen, and balance nitrous oxide, administered via endotracheal tube and artificial respiration (Model 681, Harvard Apparatus, South Natick, MA, USA). Femoral arterial and venous catheters were inserted. Inside the magnet, a MR compatible ventilator (MRI-1, CWE, Ardmore, PA, USA) was used. Arterial blood pressure was continuously monitored from a femoral artery using a strain gauge transducer (DT-XX, Viggo Spectramed, Miami, FL, USA) and recorded on a polygraph (Gould, Cleveland, OH, USA). An appropriate maintenance level of isoflurane was determined by monitoring the blood pressure response to tail pinch. Body temperature was maintained at 37°C by a servocontrolled system consisting of a rectal temperature probe and a heating blanket outside the magnet or a thermostated water jacket inside the magnet. Immobilization was implemented with 0.4 mg/kg pancuronium bromide injected intramuscularly at 60 min intervals (on the bench) or continuously infused intravenously at 0.4 mg/kg/h (delivered at 1 mL/h) inside the magnet. To ensure physiological stability, arterial blood pH and gases ($PaCO_2$, PaO_2) were measured (ABL-3, Radiometer America, Westlake, OH, USA) before surgery, at different phases of surgery, and at regular intervals during MRI; in total, typically, at 4–7 time points. With the blood volume per sample being of ≈ 65 μL, the total volume of withdrawn blood was not hemodynamically significant.

Middle Cerebral Artery Occlusion (MCAO)

In eight animals, permanent focal cerebral ischemia was produced by insertion of an intraluminal suture. The 3-0 monofilament poly-L-lysine coated nylon suture was inserted 20–21 mm through the internal carotid artery and further into the circle of Willis, occluding the middle cerebral artery (MCA) at its origin (23). In two other animals, MCA transection and bilateral common carotid artery occlusion (MCAT) was performed as described previously (17,18).

MRI

For ^{23}Na/^{1}H MRI, the animal's head was positioned inside a 5-cm-diameter, 5-cm-long dual-tuned dual-quadrature birdcage transmit/receive radiofrequency (RF) coil (24) in the animal cradle with a recirculating water bed and fittings for respiratory and anesthesia gas supply. Images were obtained on a 3 T whole body scanner (General Electric Medical Systems, Milwaukee, WI, USA) within a field of view (FOV) of 50×50×50 mm. The typical experimental timeline was:

stroke induction – scout imaging – first ADC map – multiple ^{23}Na MRI (every 5.3 min) – B_1 mapping – multiple ^{23}Na MRI – second ADC map – multiple ^{23}Na MRI.

^{1}H diffusion-weighted multislice spin-echo images (*TR*/*TE* of 2000/140 ms, in-plane resolution of 0.2 mm, eight 3.2-mm-thick slices, diffusion weighting *b*-factor values of 0, 93, 372, and 837 s/mm^2, scan time per *b*-factor was 4.7 min), with the diffusion-sensitizing gradient applied along each of the Cartesian axes, were used for reconstruction of ADC trace maps. To minimize the contribution of capillary microcirculation to ADC, all *b*-factor values were in the range governed by molecular diffusion (25). ^{23}Na MRI was performed using a three-dimensional (3D) twisted projection imaging (TPI) scheme (26) with a voxel size of 0.48 mm^3, imaging time of 5.3 min (eight transients for each of 398 projections), and the inhomogeneity correction of the B_1 field by RF mapping (27,28). An ultra-short *TE* of 0.4 ms and a long *TR* of 100 ms were used to eliminate a quantitation bias resulting from possible changes in relaxation times in ischemic brain. Cylindrical tubes containing NaCl solutions at different concentrations (0, 77, 116 and 154 mM) were placed next to animal's head and served as external position and concentration references after correction for partial ^{23}Na signal saturation in the solution due to its longer T_1 (T_1 = 60 ms, correction factor $1 - \exp(-TR/T_1)$). Tissue ^{23}Na with T_1 of 10–30 ms is fully relaxed in these conditions. The ^{23}Na MRI series typically spanned two to four hours within a 1.1- to 7.3-hour window after ischemia.

Brain Processing

After the end of MRI scanning (typically, 4.5 to 7.3 h after MCAO), rats were decapitated, and their heads were immediately frozen in dry ice and stored at –80ºC in order to preserve the spatial characteristics of the brain for further superposition and comparison with MR images. The brain was chipped out of the skull in a –20ºC cold box and mounted into the cryostat (–8ºC). Twelve to 18 samples of approximately 0.5 mg wet weight were punched from the ipsilateral and contralateral brain (19,28) at two or three coronal levels, typically between +1 and –4 mm from bregma. The micro-puncher inner diameter was 0.53 mm, the sampling depth was determined by examining coronal brain cuts taken every 40 μm, and the samples were precision-weighed using a Cahn model C-44 microbalance (ATI Orion, Boston, MA, USA). The sampling location was guided by ADC and ^{23}Na maps of the brain (Fig. 1a,b) and by the change in surface reflectivity of ischemic tissue (29). Cut-face photographs of the brain were taken at several levels, including punched surfaces before and after sampling (Fig. 1c,d). The 40-μm thick coronal sections of the brain at different levels from bregma were mounted on glass slides and digitized. The infarct size and location were

verified by reflective changes and by immunohistochemistry with microtubule-associated protein-2 (MAP2) antibody in slide-mounted brain sections (29), as shown in Fig. 1e,f. Brain sodium content was determined by emission flame photometry of punched samples at 589 nm using an IL943 flame photometer (Instrumentation Laboratory, Lexington, MA, USA).

Image Processing

Parametric ^{1}H ADC maps were generated pixel-wise by exponential fitting of the diffusion-weighted image intensity vs. the *b* value (30) in MatLab (MathWorks, Natick, MA, USA). ^{23}Na MR images were reconstructed, corrected for inhomogeneity of the B_1 field and for the non-zero noise baseline in the magnitude mode reconstruction (27), stacked in four dimensions (including the time dimension), and parametric images of the rate of ^{23}Na signal increase ('slope') were generated from the serial ^{23}Na images (by performing a pixel-wise linear regression of image intensity versus time after stroke onset) using C and C++ scripts in the UNIX environment. Selected coronal brain slices (taken every 400 μm) and histological MAP2 stained sections (taken every 800 μm) were digitized, stacked and registered using ImageJ (31) (available from: Rasband, W.S., ImageJ, U. S. National Institutes of Health, Bethesda, Maryland, USA, http://rsb.info.nih.gov/ij/, 1997–2008) to render volumetric reconstructions of the brain. MR images were aligned with histological 3D images and cut-face photographs and analyzed using AMIDE software (32). The $[Na^+]_{br}$ values were obtained after MRI calibration against flame photometry as described elsewhere (28) by placing cylindrical ROIs in the ^{23}Na images at the positions of punch voids on histological and cut-face images, as shown in Fig. 1. To characterize the rate of $[Na^+]_{br}$ accumulation and ADC deficit in ischemic brain, $[Na^+]_{br}$ and ADC data in ischemic ROIs were referenced to the corresponding time-averaged control values of homotopic ROIs.

Statistics

Parametric and nonparametric one- or two-tailed statistical tests were applied for significance of correlations and differences, independent or paired as appropriate, with a post hoc Bonferroni correction when multiple comparisons were made, using SPSS for Windows, version 14.0 (SPSS, Chicago, IL, USA). $P < 0.05$ was taken as indicating significance. The errors are presented as SD or SEM, as indicated. The number of rats reported in some of the comparisons was less than the total (ten), because not all parts of the protocol were successfully completed in all animals.

RESULTS

Physiological Monitoring

Physiological variables at different phases of the experimental protocol were in the normal range for all animals, as summarized in Table 1. Minor fluctuations in physiological variables were not accompanied by deviations in the ^{23}Na time courses. Between the animals, the ^{23}Na slope values did not correlate with mean arterial blood pressure ($P > 0.1$).

$[Na^+]$ Increase in Ischemic Brain

The ischemic lesion (as defined by the ADC deficit, changes of surface reflectivity, and MAP2 staining) involved parts of the cortex and CP, as is typical for the suture MCAO model. Therefore, the changes in $[Na^+]_{br}$ after MCAO were analyzed in the ipsilateral and homotopic contralateral frontal cortex, parietal cortex and CP (Fig. 1). ^{23}Na MRI intensity showed a linear increase in ischemic brain and no statistically significant changes in contralateral ROIs over time (Fig. 2). Within the boundaries of the infarct region, sites with an elevated rate of ^{23}Na increase (slope) were observed in all animals (Fig. 1b), either in the

cortex (n = 7) or in CP (n = 2), as shown in Table 2. The rat #9 accidentally died during scanning, and the observation time was too short (approximately 1 h) for the linear regression to reach statistical significance. The slope values at the sites of maximum slope were significantly higher than other slopes within ischemic cortex or CP in the same brain ($P < 0.005$ by paired *t*-test). The maximum slope values averaged over all animals were 22 ± 4%/h (mean ± SEM), as compared with 14 ± 1%/h in other ischemic ROIs. The mean value of maximum slope in CP was 15 ± 1%/h (rats #6 and 7), and in the cortex, 24 ± 5%/h (in other 6 rats). A chi-square test showed that the cortical location of the sites of maximum slope was associated with higher slope values at these sites ($P = 0.04$).

Comparative Mapping of ADC and ^{23}Na Slope

$[Na^+]_{br}$ accumulation in different cortical and subcortical areas quantitated by ^{23}Na MRI was juxtaposed with the ADC deficit calculated as a ratio of ipsilateral to homotopic contralateral ROIs, ADC_i/ADC_c. In contrast to the observation of 'hot spots' of $[Na^+]_{br}$ increase by ^{23}Na MRI, the ADC deficit in the ischemic area was mostly homogeneous. ADC_i/ADC_c was 0.63 ± 0.07 (mean ± SD) without statistically significant variations ($P > 0.7$) between different ischemic regions (cortex, CP, sites of maximum slope) and stable over time (except for some parts of ischemic CP in rat #6, where ADC_i/ADC_c decreased approximately from 0.8 to 0.5 between the first and second ADC mapping). Figure 1a demonstrates mostly homogeneous ADC deficit in the ischemic area. Figure 3 shows that the values of ^{23}Na slope and ADC_i/ADC_c measured within the same ischemic ROIs did not correlate either in individual brain or between the sites of maximum slope in different animals. Table 3 illustrates this point for all individual brains. In addition, the $[Na^+]_{br}$ dynamics in the individual brains was approached independently by direct measurement of $[Na^+]_{br}$ at the end of experiment using flame photometry. In this case, the correlation between ADC_i/ADC_c and $[Na^+]_{br}$ in the same ROIs (also shown in Table 3) was absent in all rats but one. The only statistically significant correlation (rat #6) was positive ($R = 0.93$), which suggested the possibility that more Na^+ accumulated in the regions with moderate ADC deficit than with the more severe ADC deficit. Thus, in the ROIs characterized as ischemic by the ADC criterion, neither the fastest $[Na^+]_{br}$ increase nor the highest $[Na^+]_{br}$ at the end of experiment were accompanied by the strongest ADC depression.

Maximum Na^+ Imbalance at the Stroke Periphery

After the borders of ischemic core were defined by ADC, MAP2 staining, and by the reflectivity changes, the site with a maximum rate of $[Na^+]_{br}$ increase within the ischemic core was identified by ^{23}Na MRI as a 3D isocontour ROI at the 90% level of the maximum slope. A position of the center of mass of this isocontour ROI was determined using a corresponding tool in AMIDE. In all 8 animals amenable to analysis (out of 10), the site of the maximum slope was located near the ischemic core periphery, i.e., within 30% of the overall lesion extension. Its positions relative to the lesion were dorsolateral (n = 3), ventral (n = 3) or caudal (n = 2). In the two other rats, the data were excluded because of motion artifacts (rat #2) and the limited extent of the ischemic area (rat #4). The average distance between the centers of mass (as determined in AMIDE) of the lesion and of the ROI of the maximum slope was 4.1 ± 0.9 mm (mean ± SEM). Figure 4 presents two examples of the maximum slope location in ischemic core periphery.

DISCUSSION

The present study demonstrated that ^{23}Na MRI is more sensitive than ADC for assessing heterogeneity within the ischemic core in an animal model of permanent focal stroke. This result is based on the systematic comparison of dynamics of Na^+ imbalances with ADC values within the ischemic core in the absence of reperfusion. The heterogeneity of these

imbalances suggests the role of collateral circulation in the physiology and pathology of ischemic stroke, because the increase in $[Na^+]_{br}$ is due to a delicate interaction of continuing Na^+ delivery through trickle flow and impaired egress from edema because of swelling. Though energy depletion is a primary cause of cytotoxic brain edema, the resulting disturbances of water and ion homeostasis are mediated by residual or collateral circulation, which act, in particular, as a source of Na^+ (17,18,33).

In agreement with earlier studies (14,16–19), a linear increase in $[Na^+]_{br}$ was observed during evolution of cerebral ischemia between 1.1 and 7.3 h after MCAO (Fig. 2). Effects of focal ischemia may vary with the brain region (22). The data showed that ischemic cortex was a more favorable location than CP for Na^+ accumulation: 1) the sites of maximum slope were found in the cortex more often (n = 7) than in CP (n = 2), and 2) the sites of maximum slope located in the cortex had typically higher slope values than the sites of maximum slope in CP. These differences may be attributable to the peculiarities in collateral circulation in the two brain regions. Even after total occlusion of main nourishing artery, the cortical pial vascular network is able to provide a collateral supply of blood flow at the border of that vascular territory (21). On the other hand, the blood supply to the subcortical CP is of the collateral-lacking “end artery” type (20). This difference might be of relevance for $[Na^+]_{br}$ increases because the higher trickle flow through the collateral network in ischemic cortex (and less trickle flow in CP) may explain the higher slope in the cortex.

The possibility of relation of the $[Na^+]_{br}$ increase to the ADC decrease was examined. No correlation was observed, however, between the slope values or $[Na^+]_{br}$ and ADC_i/ADC_c in the same ROIs, both between animals (Fig. 3) and within the same brain (Table 3). The data in Table 3 show that within the same brain, the regions of the strongest Na^+ accumulation did not coincide with the most ADC-depressed regions. Moreover, the variations in ADC_i/ADC_c within the ischemic area of the brain, although present, were not statistically significant. Several previous reports on the fall in ADC correlated with severity of brain perfusion deficit (8,10,34) owed, probably, to a better MR sensitivity: 1) at 4.7 T compared to 3 T in the present study (8,10), or 2) in a human brain vs. small rat brain (34). Thus, ^{23}Na slope mapping in the ischemic brain provided better description of the heterogeneity in the ischemic core compared to the ADC mapping in particular experimental setting of our study.

Figure 4 further demonstrates that the site of maximum slope tends to be located at the periphery of the ischemic core. Previously, in the MCAT model yielding a purely cortical stroke (17), the maximum Na^+ increase also appeared at the edge of the infarct region. ^{23}Na MRI in non-human primate focal cerebral ischemia revealed the same trend (35). This supports the concept that the increase in $[Na^+]_{br}$ occurs at a maximum rate at the site of maximum Na^+ delivery via trickle flow or, alternatively, at the site of maximum swelling and most limited Na^+ egress. Supposedly edema is more severe at the edge of the ischemic region, driven by the more available collateral flow delivering more Na^+ (33). Ion imbalances at the edges of the ischemic region manifested themselves in a more severe decrease of $[K^+]_{br}$ in gerbils (33) and in the MCAT model in rats (36). It should be underscored that the trickle flow supplying Na^+ to the developing “edge edema” is still below the ischemic threshold, so this edge region belongs to the ischemic core and must not be confused with ischemic penumbra. The presence of slightly more trickle blood supply may modulate the severity of ischemic damage.

Thus, the rate of $[Na^+]_{br}$ increase as measured by ^{23}Na MRI may serve as a complementary tool in assessing ischemic damage and treatment planning. A reliable regional quantitation of $[Na^+]_{br}$ increase in ischemia was demonstrated using ^{23}Na MRI with a small voxel size in a small animal model. It is reasonable to expect even better accuracy in the clinical setting

where the requirements to the signal-to-noise ratio imposed by the voxel size are less demanding.

In conclusion, ^{23}Na MRI revealed heterogeneity in the rate of $[Na^+]_{br}$ increase, or slope, within the ischemic core in the rat brain. The maximum rate of $[Na^+]_{br}$ accumulation was at the periphery of the ischemic core. The fastest $[Na^+]_{br}$ increase occurred preferentially in the cortex rather than CP. The accumulation of Na^+ by ^{23}Na MRI provides an enhanced physiological characterization of ischemic lesion not available by ADC.

Acknowledgments

The authors thank Jayashree Kanchana for early efforts in data processing, and Jayjayantee Dasgupta for technical support.

Contract grant sponsor: National Institutes of Health; Grant number: NS30839.

REFERENCES

1. Roberts TP, Rowley HA. Diffusion weighted magnetic resonance imaging in stroke. Eur J Radiol. 2003; 45:185–194. [PubMed: 12595102]
2. Schlaug G, Benfield A, Baird AE, et al. The ischemic penumbra: operationally defined by diffusion and perfusion MRI. Neurology. 1999; 53:1528–1537. [PubMed: 10534263]
3. Kidwell CS, Alger JR, Saver JL. Beyond mismatch: evolving paradigms in imaging the ischemic penumbra with multimodal magnetic resonance imaging. Stroke. 2003; 34:2729–2735. [PubMed: 14576370]
4. Rivers CS, Wardlaw JM, Armitage PA, et al. Do acute diffusion- and perfusion-weighted MRI lesions identify final infarct volume in ischemic stroke? Stroke. 2006; 37:98–104. [PubMed: 16322499]
5. Guadagno JV, Warburton EA, Jones PS, et al. The diffusion-weighted lesion in acute stroke: heterogeneous patterns of flow/metabolism uncoupling as assessed by quantitative positron emission tomography. Cerebrovasc Dis. 2005; 19:239–246. [PubMed: 15741718]
6. Sobesky J, Zaro WO, Lehnhardt FG, et al. Does the mismatch match the penumbra? Magnetic resonance imaging and positron emission tomography in early ischemic stroke. Stroke. 2005; 36:980–985. [PubMed: 15790950]
7. Guadagno JV, Donnan GA, Markus R, Gillard JH, Baron JC. Imaging the ischaemic penumbra. Curr Opin Neurol. 2004; 17:61–67. [PubMed: 15090879]
8. Perez-Trepichio AD, Xue M, Ng TC, et al. Sensitivity of magnetic resonance diffusion-weighted imaging and regional relationship between the apparent diffusion coefficient and cerebral blood flow in rat focal cerebral ischemia. Stroke. 1995; 26:667–675. [PubMed: 7709416]
9. Yushmanov VE, Wang L, Liachenko S, Tang P, Xu Y. ADC characterization of region-specific response to cerebral perfusion deficit in rats by MRI at 9.4 T. Magn Reson Med. 2002; 47:562–570. [PubMed: 11870844]
10. Yushmanov VE, Kharlamov A, Simplaceanu E, Williams DS, Jones SC. Differences between arterial occlusive and thrombotic stroke models with magnetic resonance imaging and microtubule-associated protein-2 immunoreactivity. Magn Reson Imaging. 2006; 24:1087–1093. [PubMed: 16997079]
11. Lee JM, Vo KD, An H, et al. Magnetic resonance cerebral metabolic rate of oxygen utilization in hyperacute stroke patients. Ann Neurol. 2003; 53:227–232. [PubMed: 12557290]
12. Geisler BS, Brandhoff F, Fiehler J, et al. Blood-oxygen-level-dependent MRI allows metabolic description of tissue at risk in acute stroke patients. Stroke. 2006; 37:1778–1784. [PubMed: 16741186]
13. Sun PZ, Zhou J, Sun W, Huang J, van Zijl PC. Detection of the ischemic penumbra using pH-weighted MRI. J Cereb Blood Flow Metab. 2007; 27:1129–1136. [PubMed: 17133226]

14. Thulborn KR, Gindin TS, Davis D, Erb P. Comprehensive MRI protocol for stroke management: tissue sodium concentration as a measure of tissue viability in non-human primate studies and in clinical studies. Radiology. 1999; 213:156–166. [PubMed: 10540656]
15. Lin SP, Song SK, Miller JP, Ackerman JJ, Neil JJ. Direct, longitudinal comparison of ^{1}H and ^{23}Na MRI after transient focal cerebral ischemia. Stroke. 2001; 32:925–932. [PubMed: 11283393]
16. Boada, FE.; LaVerde, GC.; Jungreis, C.; Nemoto, E.; Tanase, C.; Hancu, I. Loss of cell ion homeostasis and cell viability in the brain: What sodium MRI can tell us. In: Ahrens, ET., editor. In vivo Cellular and Molecular Imaging. Philadelphia: Academic Press; 2005. p. 77-101.
17. Jones SC, Kharlamov A, Yanovski B, et al. Stroke onset time using sodium MRI in rat focal cerebral ischemia. Stroke. 2006; 37:883–888. [PubMed: 16424376]
18. Wang Y, Hu W, Perez-Trepichio AD, et al. Brain tissue sodium is a ticking clock telling time after arterial occlusion in rat focal cerebral ischemia. Stroke. 2000; 31:1386–1392. [PubMed: 10835461]
19. Yushmanov VE, Kharlamov A, Boada FE, Jones SC. Monitoring of brain potassium with rubidium flame photometry and MRI. Magn Reson Med. 2007; 57:494–500. [PubMed: 17326173]
20. Shigeno T, McCulloch J, Graham DI, Mendelow AD, Teasdale GM. Pure cortical ischemia versus striatal ischemia. Surg Neurol. 1985; 24:47–51. [PubMed: 4012559]
21. Rubino GJ, Young W. Ischemic cortical lesions after permanent occlusion of individual middle cerebral artery branches in rats. Stroke. 1988; 19:870–877. [PubMed: 2455367]
22. Garcia JH, Liu KF, Ho KL. Neuronal necrosis after middle cerebral artery occlusion in Wistar rats progresses at different time intervals in the caudoputamen and the cortex. Stroke. 1995; 26:636–642. [PubMed: 7709411]
23. Belayev L, Alonso OF, Busto R, Zhao W, Ginsberg MD. Middle cerebral artery occlusion in the rat by intraluminal suture. Neurological and pathological evaluation of an improved model. Stroke. 1996; 27:1616–1622. [PubMed: 8784138]
24. Shen GX, Boada FE, Thulborn KR. Dual-frequency, dual-quadrature, birdcage RF coil design with identical B_1 pattern for sodium and proton imaging of the human brain at 1.5 T. Magn Reson Med. 1997; 38:717–725. [PubMed: 9358445]
25. Le Bihan D. Magnetic resonance imaging of perfusion. Magn Reson Med. 1990; 14:283–292. [PubMed: 2345508]
26. Boada FE, Gillen JS, Shen GX, Chang SY, Thulborn KR. Fast three dimensional sodium imaging. Magn Reson Med. 1997; 37:706–715. [PubMed: 9126944]
27. Boada FE, Gillen JS, Noll DC, Shen GX, Chang SY, Thulborn KR. Data acquisition and postprocessing strategies for fast quantitative sodium imaging. Int J Imaging Syst Technol. 1997; 8:544–550.
28. Yushmanov VE, Kharlamov A, Yanovski B, LaVerde GC, Boada FE, Jones SC. Sodium mapping in focal cerebral ischemia in the rat by quantitative ^{23}Na MRI. J Magn Reson Imaging. in press.
29. Kharlamov A, Kim DK, Jones SC. Early visual changes in reflected light on non-stained brain sections after focal ischemia mirror the area of ischemic damage. J Neurosci Methods. 2001; 111:67–73. [PubMed: 11574121]
30. Le Bihan D, Breton E, Lallemand D, Grenier P, Cabanis E, Laval-Jeantet M. MR imaging of intravoxel incoherent motions: application to diffusion and perfusion in neurologic disorders. Radiology. 1986; 161:401–407. [PubMed: 3763909]
31. Abramoff MD, Magelhaes PJ, Ram SJ. Image processing with ImageJ. Biophotonics International. 2004; 11:36–42.
32. Loening AM, Gambhir SS. AMIDE: a free software tool for multimodality medical image analysis. Mol Imaging. 2003; 2:131–137. [PubMed: 14649056]
33. Kato H, Kogure K, Sakamoto N, Watanabe T. Greater disturbance of water and ion homeostasis in the periphery of experimental focal cerebral ischemia. Exp Neurol. 1987; 96:118–126. [PubMed: 3556505]
34. Lin W, Lee JM, Lee YZ, Vo KD, Pilgram T, Hsu CY. Temporal relationship between apparent diffusion coefficient and absolute measurements of cerebral blood flow in acute stroke patients. Stroke. 2003; 34:64–70. [PubMed: 12511752]

35. LaVerde, GC.; Jungreis, CA.; Nemoto, E.; Kharlamov, A.; Jones, SC.; Boada, FE. Serial sodium MRI during non-human primate focal brain ischemia. Berlin, Germany. Proceedings of the Joint Annual Meeting ISMRM-ESMRMB; 2007; p. 506

36. Kharlamov A, Yushmanov VE, Jones SC. Prominent decrease of brain tissue K^+, $[K^+]_{br}$, in the peripheral regions of ischemic core evaluated by quantitative histological potassium staining. J Cereb Blood Flow Metab. 2007; 27 suppl S1 BP53-7W; doi: 10.1038/jcbfm.2007.100.

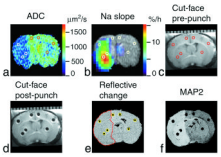

Figure 1.

Region-of-interest (ROI) analysis of Na^+ accumulation and ADC deficit in a rat brain after MCAO. Coronal images of the brain (at approximately bregma – 0.4 mm) of the rat #6 are shown. (**a**) ADC map where ADC < 500 $\mu m^2/s$ in the ischemic area (left-hand side of the image). (**b**) Pseudocolor-coded parametric image of the rate of ^{23}Na signal increase ('slope') superimposed over the grayscale ^1H spin-echo MR image as an anatomic reference. (**c**) Cut-face photograph of the brain in the cryostat before sampling and (**d**) after sampling showing punch holes. A millimeter scale is shown at the top. (**e**) Cross-section of the 3D reconstruction of the brain from the 40-μm-thick slices cut at 4.4 h post MCAO. The change in surface reflectivity of ischemic tissue shows the infarct location (outlined by a red dotted line). Cylindrical ROIs (yellow circles) were placed over the punch holes. (**f**) The absence of staining in the MAP2-stained slice indicates the ischemic lesion. Reference tubes with NaCl solutions were external to the rat head in the magnet and are not shown in MR images. ROIs defined in (e) by their correspondence to the punch positions are shown in images (a–c) as white or colored circles. The images were aligned and analyzed using AMIDE software. Punch samples were analyzed using emission flame photometry.

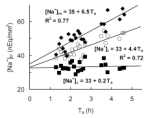

Figure 2.

Na^+ accumulation in a typical ischemic brain monitored by ^{23}Na MRI. $[Na^+]_{br}$ and corresponding linear regressions are shown for the ROIs in ischemic cortex ($[Na^+]_i$, circles), homotopic normal cortex ($[Na^+]_c$, squares), and the site of the maximum slope ($[Na^+]_m$, diamonds) in the rat #5. T_a, time after MCAO.

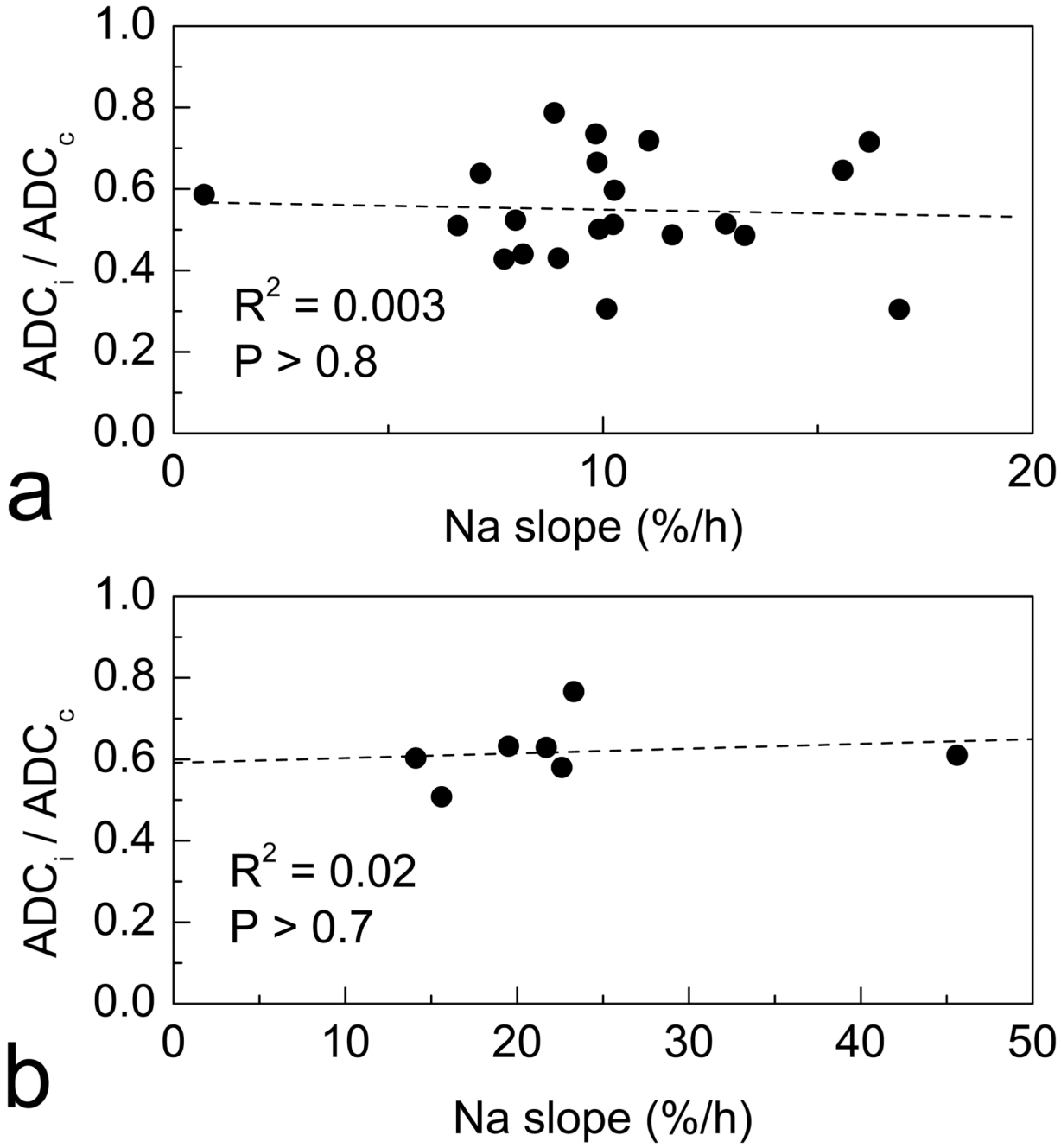

Figure 3.

^{23}Na slope (the rate of $[Na^+]_{br}$ increase) and ADC deficit (ADC ratio of ipsilateral to homotopic contralateral ROIs, ADC_i/ADC_c) in the same brain ROIs in ischemia. (**a**) In the typical brain (rat #6), ADC deficit shows no correlation with slope in ROIs characterized as ischemic by ADC (i.e., $ADC_i/ADC_c < 0.8$). (**b**) ADC deficit in the ROIs of maximum slope of different rats shows no correlation with the maximum slope values. Each data point corresponds to an individual animal for which both parameters were available (n = 7).

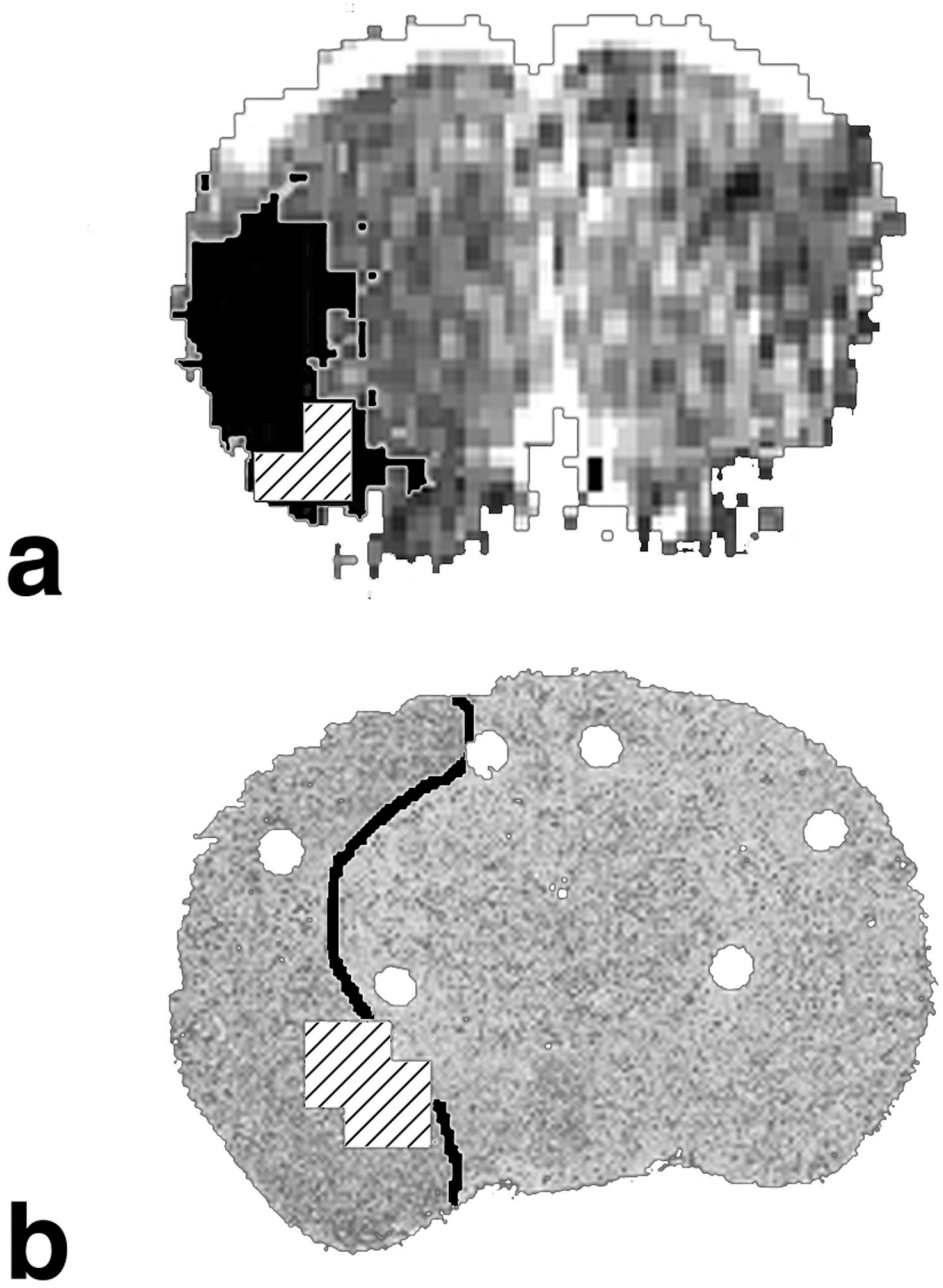

Figure 4.

Two examples of Na^+ accumulation at the periphery of the focal stroke in the rat. ROIs of maximum slope were defined by ^{23}Na MRI at an isocontour level of 90% of the maximum slope and are shown as hatched areas. (**a**) Rat #7: coronal ADC image with the ischemic region (black mask) defined as ADC < 500 $\mu m^2/s$ in the ipsilateral (left) hemisphere. (**b**) Rat #6: coronal section of the 3D reconstruction from thin slice brain images, which was aligned with brain MRI. The ischemic region (outlined) was defined by the surface reflectivity changes. ROIs of maximum slope correspond to the slope ranges of 13.5 to 15.0%/h (a) and 14.4 to 16.0%/h (b).

Table 1

Physiological variables at three phases of the protocol

	MABP(mm Hg)	pH	p_aCO_2 (mm Hg)	p_aO_2 (mm Hg)
Before MRI	109 ± 10	7.38 ± 0.07	30 ± 10	90 ± 20
Start of ^{23}Na MRI	101 ± 9	7.25 ± 0.09	30 ± 13	120 ± 64
End of experiment	90 ± 11	7.27 ± 0.05	40 ± 11	100 ± 77

Mean ± SD, n = 10.

MABP, mean arterial blood pressure; pH, arterial blood pH; p_aCO_2 and p_aO_2, partial CO_2 and O_2 pressure in arterial blood, respectively.

Table 2

Maximum ^{23}Na slopes observed after MCAO

Rat #	Ischemia model	T_d (h)[a]	Maximum slope location	Maximum slope (%/h)	R^2[b]	P[b]
1	MCAT	3.7	cortex	23 ± 6	0.59	< 0.003
c_2	MCAT	4.9	NA	NA	NA	NA
3	suture	6.0	cortex	10 ± 1	0.78	< 0.0001
4	suture	5.0	cortex	46 ± 2	0.97	< 0.0001
5	suture	5.1	cortex	20 ± 1	0.94	< 0.0001
6	suture	4.5	CP	16 ± 1	0.92	< 0.0001
7	suture	7.3	CP	14 ± 2	0.82	< 0.0001
8	suture	5.3	cortex	22 ± 1	0.96	< 0.0001
d_9	suture	2.5	cortex	-	-	> 0.1
10	suture	5.3	cortex	23 ± 3	0.82	< 0.0001

[a] T_d, duration of the experiment after MCAO.

[b] Correlation coefficient (R^2) and statistical significance (P, for the slope difference from zero) of the linear fit.

[c] The ^{23}Na MRI slope data were excluded because of the movement in the animal holder assembly.

[d] Fit parameters are not shown as lacking statistical significance.

NA = not available.

Table 3

ADC deficit (defined as ADC_i/ADC_c) and Na^+ accumulation in individual brains[a]

Rat #[b]	ADC_i/ADC_c vs. Slope		ADC_i/ADC_c vs. $[Na^+]_{EFP}$	
	R	P	R	P
1	0.20 ± 0.15	> 0.6	NA	NA
2	NA	NA	0.54 ± 0.09	> 0.3
4	−0.80 ± 0.04	> 0.1	0.30 ± 0.06	> 0.7
5	0.60 ± 0.13	> 0.1	−0.70 ± 0.11	> 0.07
6	−0.05 ± 0.14	> 0.8	0.93 ± 0.04	< 0.05*
7	−0.20 ± 0.13	> 0.6	NA	NA
8	0.55 ± 0.09	> 0.4	0.58 ± 0.09	> 0.4
9[c]	-	-	0.40 ± 0.10	> 0.5
10	0.09 ± 0.16	> 0.8	−0.05 ± 0.18	> 0.9

[a] Na^+ accumulation was characterized either by the $[Na^+]_{br}$ increase rate measured by MRI (Slope, left columns) or, independently, by $[Na^+]_{br}$ at the end of experiment as measured directly by emission flame photometry ($[Na^+]_{EFP}$ right columns). The data were obtained from ROIs characterized as ischemic by ADC (i.e., $ADC_i/ADC_C < 0.8$). R, correlation coefficient ± SD; P, statistical significance of the correlation.

[b] For the rat #3, ADC data were unavailable.

[c] Slope values are not statistically significant.

* Statistically significant.

NA = not available.